Supplementary on-line information

Supplemental Text

Methods

Generation of Transgenic Mice by GCN2.KO4 targeting

The 5' homology arm was a 6329 base pair genomic Xba1-EcoR1 fragment terminating 147 base pairs upstream of exon 12. It was ligated into a pBS plasmid containing a thymidine kinase (TK) negative selection cassette. A double-stranded oligonucleotide with EcoR1 linkers containing a *loxP* site was introduced into the EcoR1 site. This 5' *loxP* site thus flanks exon 12 on its 5'. The 3' homology arm was recovered as a PCR fragment whose 5' end is the aforementioned genomic EcoR1 site and whose 3' end is in the 17th codon of exon 14 at a Kpn1 site introduced by the oligonucleotide used in the PCR. This 4023 base pair fragment was inserted at the EcoR1-Kpn1 sites of the aforementioned pBS plasmid. The *loxP*-flanked Neo^R selection cassette was inserted into the intronic Nhe1 site 530 base pairs 3' of exon 12. W4 ES (Taconic, Germantown, NY) cells were transfected with the targeting vector, linearized at the Kpn1 site and homologous recombination was confirmed by PCR and Southern blotting. The targeted ES cells were transfected transiently with Cre-recombinase expression plasmids and derivative clones that had recombined across the 2 *loxP* sites flanking the Neo^R selection cassette (GCN2.KO4c). In addition, clones that had recombined across all three *loxP* sites (GCN2.K04ex) were isolated. Thus, the neomycin resistance marker was excised by recombination at the flanking lox P sites. This eliminates potential gain-of-function features due to the presence of the active PGK promoter embedded in the GCN2 gene. In addition to deletion of the essential exon 12, splicing of exon 11 to exon 13 is predicted

to disrupt the reading frame of the mRNA and to introduce multiple stop codons that would destabilize the mRNA. GCN2.K04ex allele was used where an 1101 base pair fragment that encompasses exon 12 was deleted. The mutant and corresponding WT alleles are detected by a three-primer PCR assay in which mGCN2.15S (5'-TCTCCC AGCGGAATCCGCACATCG-3') and mGCN2.4AS (5'-ATCCAGGCGTTGTAGTAGC GCACA-3') give a WT band of 374 bases and mGCN2.15S and mGCN218AS (T GCC ACT GTC AGA ATC TGA AGC AGG) give a 603 base-pair fragment from the deleted allele. The 1665 base pair fragment derived from the WT allele by amplification between mGCN2.15S and mGCN2.18AS is occasionally also detected in this assay.

Fear Conditioning

Mice were handled for 3-4 days before the start of the experiment. They were then habituated to two distinct contexts for 20 min for 3 days. The habituation sessions within a day were separated by at least 4 hours. Training consisted of two pairings of a tone (2800 Hz, 85 db, 30 s) with a co-terminating foot-shock (0.7 mA, 2 s). The first tone onset was applied 120 s after animals were placed in the conditioning chamber. Mice remained in the conditioning context for an additional minute after the end of the second pairing, at which point they were returned to their home cage. All mice were tested 1 and 10 days later for freezing to the tone (using a chamber they had not been conditioned in) and to the training context in a counterbalanced manner. For auditory fear conditioning, 2 min after being placed in the chamber (pre-CS period), the tone was played for 3 min. Mice were returned to their cages 30 s after the end of the tone. Assaying contextual fear conditioning entailed placing the animals in the conditioning context for 5 min. For all tests, at 5 s intervals, each mouse was judged as either freezing (immobility with the

exception of respiration) or not freezing. Indices of memory are expressed as the percent of 5 sec intervals in which freezing was observed.

Results

Basal synaptic transmission is unaltered in slices from *GCN2 -/-* mice

Synaptic transmission was studied at synapses made by Schaffer collateral and commissural fibers on apical dendrites of hippocampal pyramids in the CA1 stratum radiatum. Field excitatory postsynaptic potentials (fEPSPs) were obtained by stimulating and recording in the stratum radiatum. Basal synaptic transmission did not differ between slices from WT and mutant mice (supplementary Fig. 4). In particular, there was no significant difference in the input-output relation of fEPSPs as a function of stimulus intensity (supplementary Figs. 4A and B). In addition, neither paired-pulse facilitation (PPF) (supplementary Fig. 4C) - a presynaptically mediated short-term enhancement of transmission - nor the presynaptic fiber volley amplitude (supplementary Fig. 4D) were altered in slices from *GCN2 -/-,* as compared to WT slices. In addition, the peak amplitude in field potentials in response to the tetanus (supplementary Fig. 4E) was normal in *GCN2 -/-* as compared to WT slices. Taken together, these data indicate that both presynaptic and postsynaptic functions are intact in *GCN2 -/-* mice.

LTD. To determine whether other forms of synaptic plasticity are altered in *GCN2 -/-* mice, we studied long-term depression (LTD) induced by a low-frequency stimulation protocol (LFS) [1]. Stimulation at 1 Hz for 15 min induced a similar depression in brain slices from WT and *GCN2 -/-* mice (supplementary Fig. 6A; at 60 min, 71.3 ± 5.9% for WT slices vs. 75.9 ± 4.8% for *GCN2 -/-* slices, $p > 0.05$). Synaptic depression induced by DHPG, an agonist of group I mGluRs, was also examined [2]. Perfusion with

50 μM DHPG produced a similar LTD in both brain slices from WT and *GCN2 -/-* mice (supplementary Fig. 6B; 80.0 ± 10.8% for WT slices vs. 79.9 ± 6.6% for *GCN2*-/- slices, $p > 0.05$). These results demonstrate that slices from *GCN2 -/-* mice exhibit normal LTD. This supports the notion that the GCN2 deletion engenders a characteristic deficit in a specific form of synaptic plasticity.

Fear conditioning

Contextual. The order of tone and context presentations for each memory test was counterbalanced within groups. As there were no differences in counterbalancing (p's > 0.05), the data were merged across the appropriate conditions. For example, the data for auditory fear conditioning from animals that had the auditory test before and after the contextual freezing test were combined. The ANOVA comparing freezing scores during the two min period prior to the first shock (pre-shocks) and the one min period following the last shock (post-shocks) between WT vs. *GCN2 -/-* mice revealed no significant interaction ($F < 1$). Furthermore, although there was no main effect of Group ($F(1, 12) = 1$, $p > 0.05$), there was a significant main effect of freezing during the pre- vs. post-shocks periods ($F(1,12) = 133$, $p < 0.05$). These analyses demonstrate that there were no differences between the groups and that both acquired contextual fear conditioning. In contrast, *GCN2 -/-* mice showed a deficit 1 and 10 days after training (Fig. 3A). A repeated measure ANOVA on the performance of WT and *GCN2 -/-* mice on the 1 and 10 day test revealed no significant interaction ($F <1$), nor any significant main effect of Test ($F < 1$). Importantly, there was a significant group effect ($F (1,12) = 90$, $p < 0.05$).

Auditory. *GCN2 -/-* mice show an intact auditory fear conditioning (Fig. 3B). A repeated measures ANOVA on the freezing scores of the 1 or 10 day test between WT and

GCN2-/- revealed no significant interaction ($F < 1$), no main effect of Group ($F < 1$), nor a main effect of Test ($F < 1$). Moreover, performance on auditory fear conditioning was not compromised by differential levels of baseline freezing to the context during the tests as there were no differences between WT and mutant mice on pre-CS freezing (p's > 0.05). Furthermore, there was no main effect of group ($F(1,12) = 1.4$, $p > 0.05$) demonstrating that the groups behaved comparably over the training session. Both groups acquired auditory fear conditioning as there was a significant main effect of training tones ($F(1,12) = 7$, $p < 0.05$).

Discussion

We show for the first time that a well established translational regulator, GCN2, plays a critical role in synaptic plasticity, learning and memory. Although a global knockout mouse was used in this study, several lines of evidence rule out non-specific changes. First, there is no evidence of hippocampal degeneration in *GCN2 -/-* mice. Second, the changes in synaptic plasticity are highly specific based on several criteria: slices from *GCN2 -/-* mice exhibit a sustained LTP induced with a single tetanic train, impaired L-LTP elicited with 4 tetanic trains and forskolin, but normal basal transmission, paired pulse plasticity and LTD. Therefore, this novel phenotype represents a dissociation of the three processes: E-LTP, L-LTP and LTD. Third, *GCN2 -/-* mice exhibit impaired behavior in two hippocampus-dependent tasks, the Morris water maze (3T/d) and contextual fear conditioning when acquired with two trials. In sharp contrast, they display normal performance on non-hippocampus-dependent tasks such as the visible platform version of the water maze and auditory fear conditioning. The ability to acquire fear auditory conditioning suggests that GCN2 is not necessary for plasticity in

the amygdala, the putative site of fear learning and memory [3]. Moreover, *GCN2 -/-* mice show an enhanced spatial memory on the Morris water maze task when a weak training protocol (1 T/d) is administered. These data underscore the specificity of the behavioral impairment with multiple training protocols. Thus, the behavioral phenotypes are in accordance with the LTP effects observed with 1 and 4 tetanic trains. Furthermore, the specificity of the phenotype extends to certain other forms of plasticity and memory processes that are dependent on translation. For instance, *GCN2-/-* mice show normal mGluR induced LTD and enhanced spatial memory induced with 1 T/d, both of which depend on translation [4,5].

We propose that GCN2 regulates the switch from short-term to long-term memory. Our model is consistent with the report that inhibition of an ATF4 homologue, the ApCREB-2 repressor, is associated with enhanced synaptic facilitation in *Aplysia* [6]. Mice expressing an inducible inhibitor of ATF4 and C/EBP proteins, EGFP-AZIP, are similar to *GCN2 -/-* mice in that a single tetanic train elicits L-LTP in hippocampal slices [5]. A further similarity is that for both EGFP-AZIP and *GCN2 -/-* mice, a weak training protocol is sufficient for the acquisition of long-term memory. However, in the EGFP-AZIP (unlike *GCN2 -/-)* mice, there was no impairment of either L-LTP or spatial learning induced with strong training protocols. One possible explanation for this difference is that EGFP-AZIP targets ATF4 as well as C/EBP proteins [5]. It is also possible that in the absence of GCN2, the expression of additional inhibitory factors, other than ATF4, is induced in response to strong stimulation.

Supplementary Figure legends

Fig. 1. Generation and Characterization of the *GCN2 -/-* mice.

A) Scheme of the region encompassing exon VII-XVII of the mouse *GCN2* locus (*EIF2AK4*). The *loxP* recombination sites in the targeting vector are depicted by triangles and the NEO resistance cassette, transcribed in an orientation opposite to GCN2, is depicted by the black rectangle. In the mutant locus (GCN2.KO4), recombination between the 5' and 3' *loxP* sites results in deletion of exon 12, which encodes residues critical for ATP binding in the kinase domain. Splicing of exon 11 to exon 13 is predicted to disrupt the reading frame of the mRNA and introduce multiple stop codons which are expected to destabilize the mRNA. **B)** Characterization of GCN2 protein expression. WT and *GCN2 -/-* hippocampal (lanes 1 and 2) and MEF (lanes 3 and 4) extracts were immunoprecipitated with α-N-term and α-C-term GCN2 antibodies. After SDS 15%-PAGE, blots were probed with affinity-purified-N-term and C-term antibodies as previously described (*11*). **C)** Distribution of GCN2 as visualized by immunohistochemistry in the forebrain section of WT (upper panel) and *GCN2 -/-* (lower panel) mice. GCN2 is expressed predominantly in the hippocampal CA1 region and the dentate gyrus, and to a lesser degree in CA3 (Fig. 1C, upper panel). No signal was detected in the brain of *GCN2 -/-* mice (Fig. 1C, lower panel).

Fig. 2. Expression of GCN2 in adult brain. *In situ* hybridization using an antisense riboprobe (all panels except for D where the cortex was probed with a sense probe) against exon 12 of mouse GCN2 was performed on dry films (A, WT and B, *GCN2 -/-*) and on emulsions of neuronal structures from cortex (C), hippocampus (E) and cerebellum (F, thick and thin arrows indicate granular layer and Purkinje cell neurons respectively; D, white arrows indicate neuronal position). GCN2 is expressed

predominantly in the hippocampal CA1 and CA3 regions and the dentate gyrus (Fig. 2A). As expected, no *GCN2* mRNA expression is detected in *GCN2 -/-* mice (Fig. 2B). Abbreviations: Cb, cerebellum; CC, corpus callosum; Cx, cerebral cortex; DG, dentate gyrus; Hip, hippocampus; Hy, hypothalamus; MB, mammillary bodies; OL, olfactory lobe; Str, striatum. Magnifications: x 4.4 (in A,B) and x 1260 (in C-F). Bar (in F) = 10 μm.

Fig. 3. Lack of gross structural abnormalities in *GCN2 -/-* mice. Left and right panels represent sections from two different Nissl stained mouse brains.

Fig. 4. Normal basal synaptic transmission in *GCN2 -/-* mice.

A) Imput-output curves show similar field excitatory postsynaptic potentials (fEPSPs) slopes over a range of stimulus intensities for both *GCN2 -/-* and control (WT) littermates. **B)** Representative traces of fEPSPs are similar for *GCN2 -/-* and WT mice. **C)** Comparison of paired-pulse facilitation (PPF) in *GCN2 -/-* and WT slices. Data are presented as the mean (± SEM) facilitation of the second response relative to the first response. **D)** Imput-output relation of fEPSPs as a function of pre-synaptic fiber volley size was similar for WT and *GCN2-/-* slices. **E)** Superimposed mean fEPSPs during tetanization (100 Hz, 1s) show no significant difference between *GCN2 -/-* and WT slices ($p > 0.05$).

Fig. 5. Properties of LTP induced in slices from *GCN2 -/-* mice.

A) Two independent inputs S1 and S2 to the same neuronal population were alternatively stimulated. One train of high frequency stimulation (100 Hz for 1s) in S1 elicited a robust and sustained LTP, whereas test stimulation (0.033 Hz) in S2 revealed stable recording during the entire experiment session in the same slice. Gray diamonds represent a control

stimulated synaptic input, S2, that remained stable at baseline level for the entire experimental session. **B)** E-LTP elicited in WT slices is not affected by translation, transcription or PKA inhibitors. E-LTP produced in WT slices is not affected by anisomycin (ANISO, 40μM; at 180 min, LTP was 110.4 ± 7.2% for control slices and 112.8 ± 5.6 % for treated slices, $p > 0.05$), actinomycin D (ACTD, 40μM; at 180 min, LTP was 110.4 ± 7.2% for control slices and 119.9 ± 15.1% for treated slices, $p > 0.05$) or the PKA inhibitor KT5720 (1μM; at 180 min, 110.4 ± 7.2% for controls vs. 130.0 ± 9.1% for treated slices, $p > 0.05$). **C)** Forskolin-induced L-LTP (50μM) was impaired in *GCN2 -/-* slices (at 240 min 136.6 ± 9.4% for WT vs. 100.9 ± 12.9% for *GCN2 -/-* slices , $p < 0.05$). **D)** Five minutes after a single train of 100 Hz, stimulation at 5 Hz depotentiated LTP elicited in WT slices, whereas the sustained LTP induced in *GCN2 -/-* slices was resistant to depotentiation (at 60 min, 111.1 ± 12.5% for WT slices vs. 179.8 ± 24.1% for *GCN2 -/-* slices, $p < 0.05$). Representative fEPSP recordings from time points (a) and (b) are shown for each condition.

Fig. 6. LTD is normal in GCN2 -/- slices.

A) WT and *GCN2 -/-* slices showed no significant difference in LTD induced by 1 Hz stimulation. **B)** LTD induced by 50μM DHPG was normal in both WT and *GCN2 -/-* slices.

Fig. 7. L-LTP but not E-LTP-inducing protocols regulate GCN2 activity.

Hippocampal slices were either test stimulated (0.033 Hz) or stimulated with 1 or 4 trains of HFS (n =4). Extracts were prepared from CA1 region from slices that had been frozen 15 minutes after either control stimulation or 4 trains of 100 Hz stimulation. Western-

Blotting shows that unlike 1 train (B), 4 trains (A) of HFS decreases GCN2 and eIF2α phosphorylation.

Supplementary References.

1. O'Dell, T. J. & Kandel, E. R. Low-frequency stimulation erases LTP through an NMDA receptor-mediated activation of protein phosphatases. *Learn Mem* **1**, 129-39 (1994).
2. Palmer, M. J., Irving, A. J., Seabrook, G. R., Jane, D. E. & Collingridge, G. L. The group I mGlu receptor agonist DHPG induces a novel form of LTD in the CA1 region of the hippocampus. *Neuropharmacology* **36**, 1517-32 (1997).
3. LeDoux, J. E. Emotion circuits in the brain. *Annu Rev Neurosci* **23**, 155-84 (2000).
4. Huber, K. M., Kayser, M. S. & Bear, M. F. Role for rapid dendritic protein synthesis in hippocampal mGluR-dependent long-term depression. *Science* **288**, 1254-7 (2000).
5. Chen, A. et al. Inducible enhancement of memory storage and synaptic plasticity in transgenic mice expressing an inhibitor of ATF4 (CREB-2) and C/EBP proteins. *Neuron* **39**, 655-69 (2003).
6. Bartsch, D. et al. Aplysia CREB2 represses long-term facilitation: relief of repression converts transient facilitation into long-term functional and structural change. *Cell* **83**, 979-92 (1995).

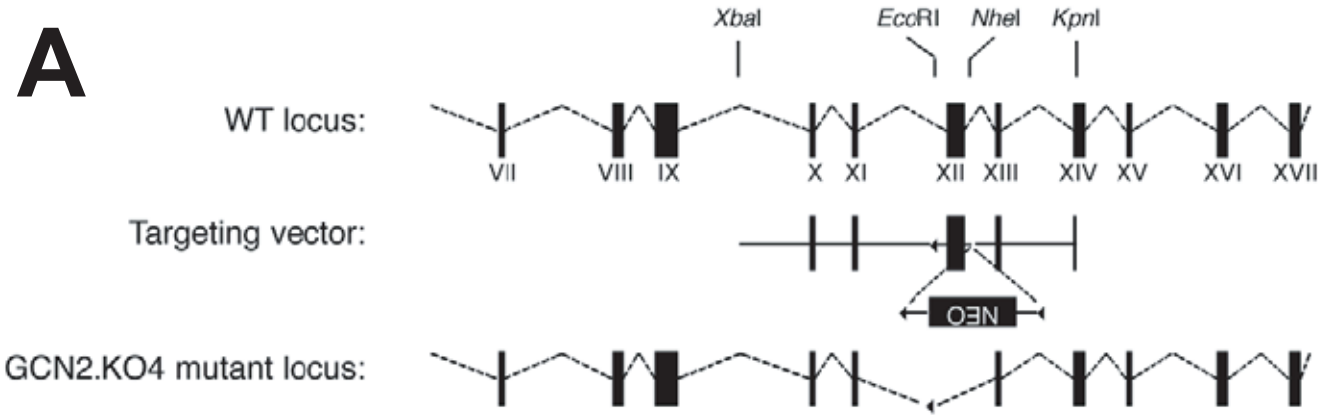
A
XbaI
EcoRI
NheI
KpnI
WT locus:
VII
VIII
IX
X
XI
XII
XIII
XIV
XV
XVI
XVII
Targeting vector:
NEO
GCN2.KO4 mutant locus:

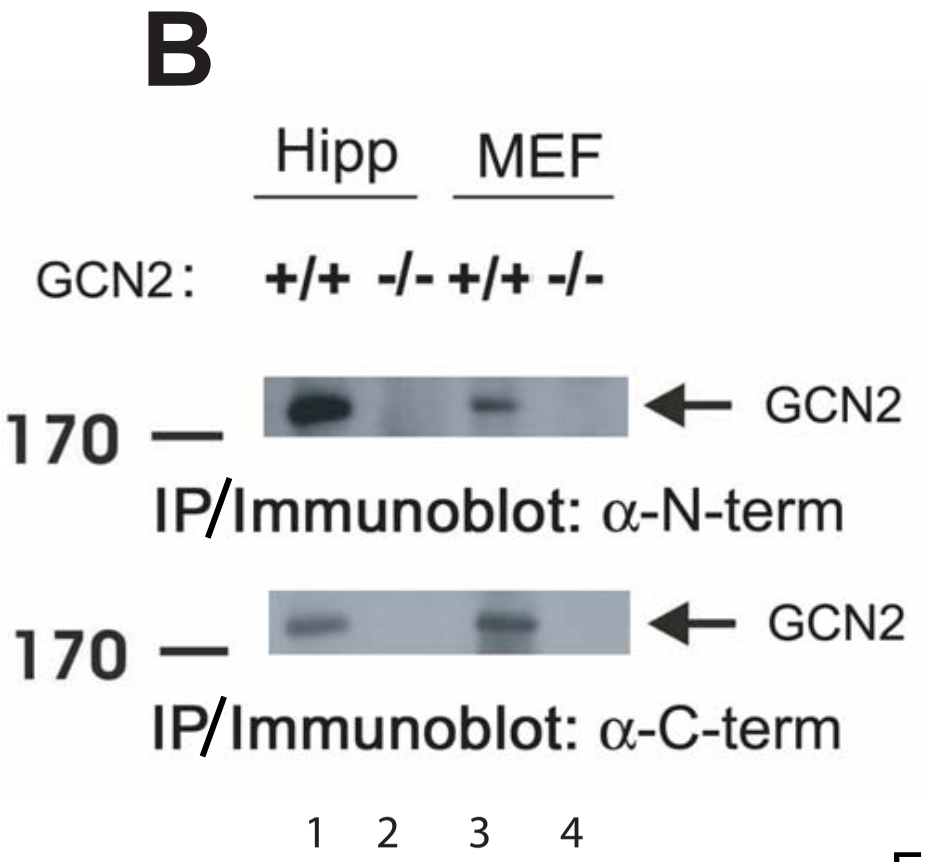
B
Hipp
MEF
GCN2: +/+ -/- +/+ -/-
170
GCN2
IP/Immunoblot: α-N-term
170
GCN2
IP/Immunoblot: α-C-term
1 2 3 4

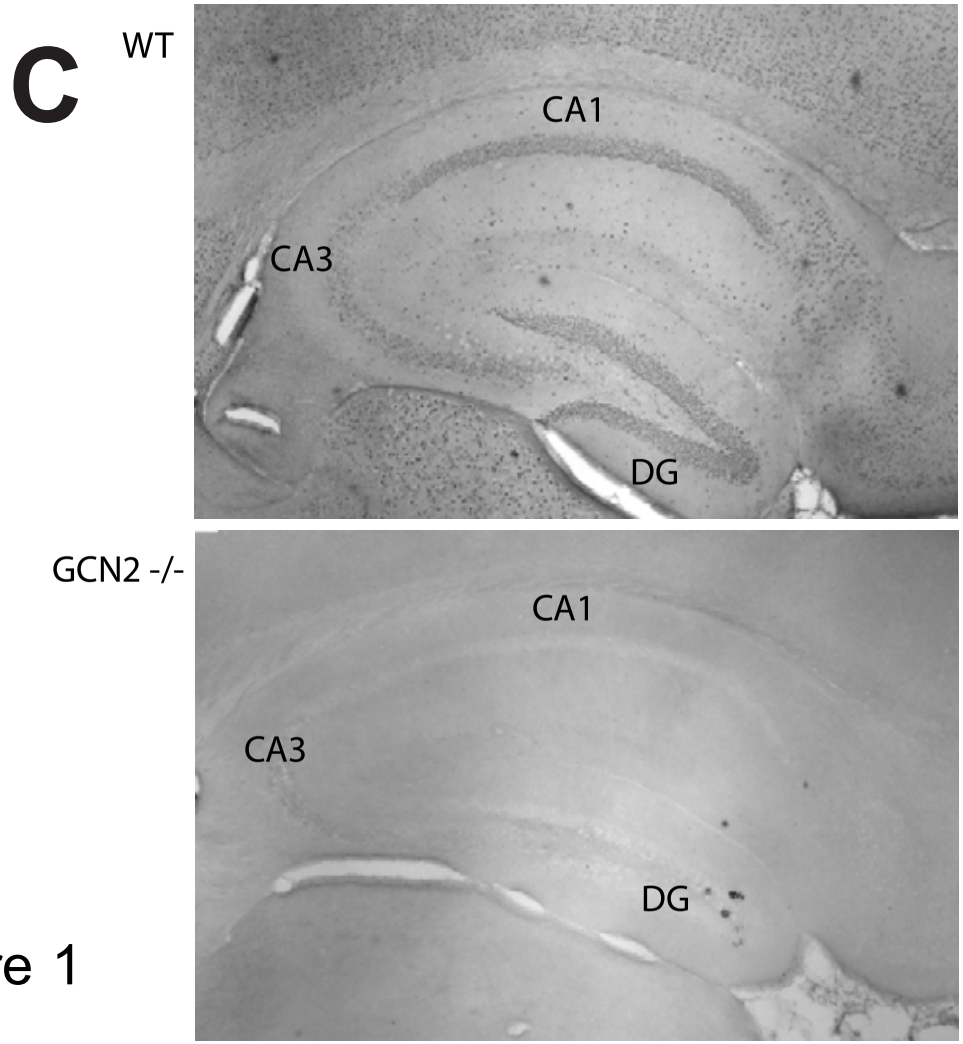
C
WT
CA1
CA3
DG
GCN2 -/-
CA1
CA3
DG

Figure 1

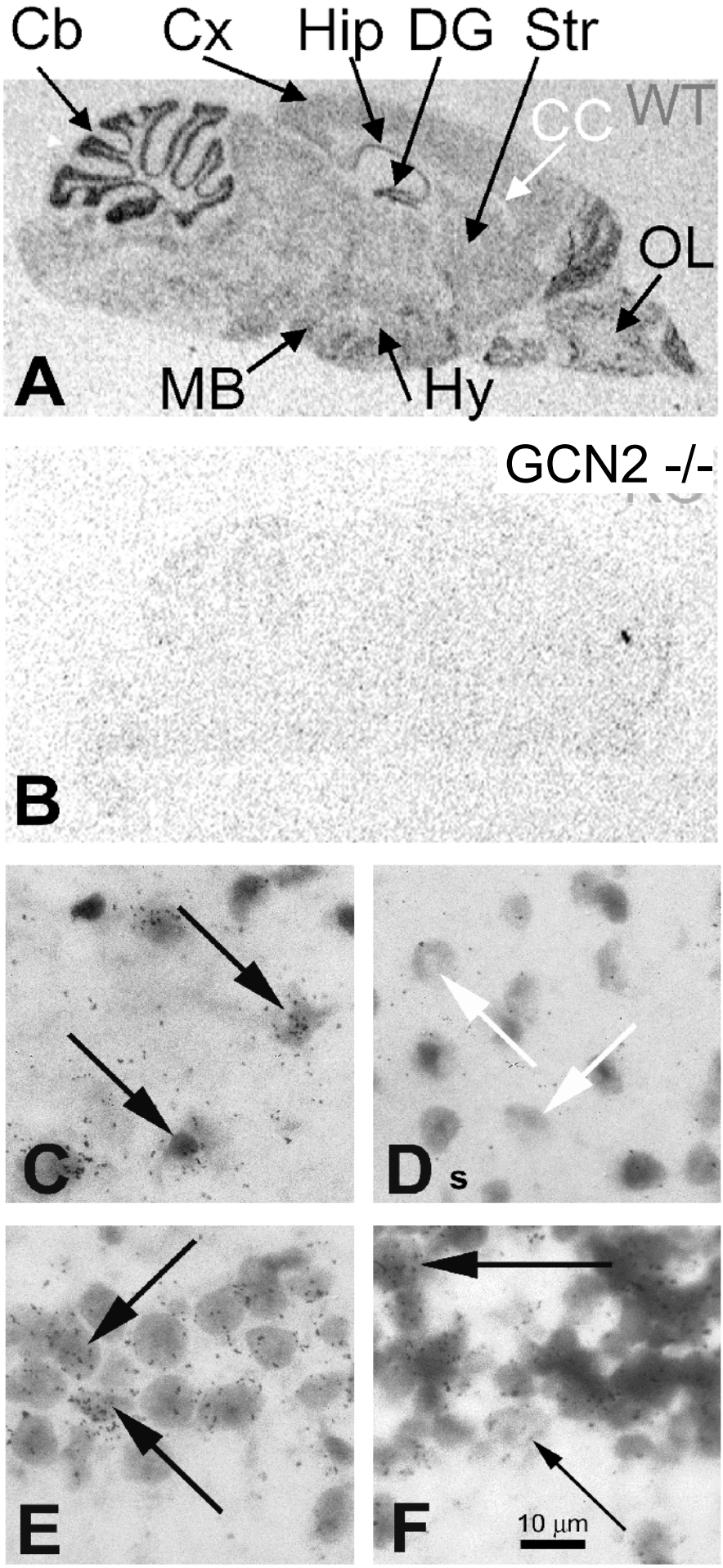

Figure 2

Nissl

WT

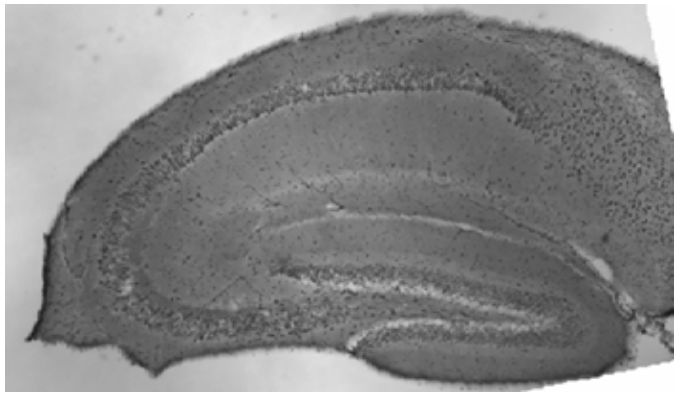

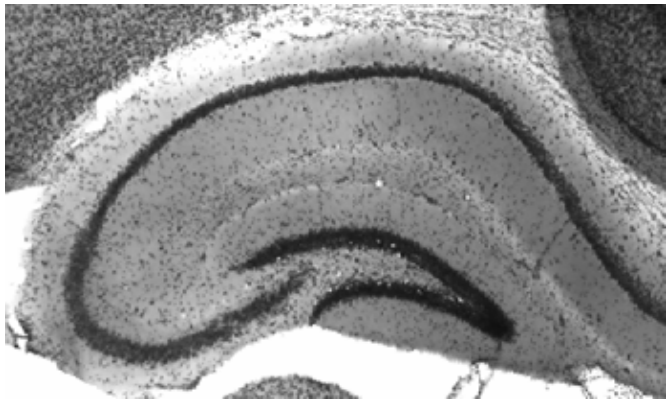

GCN2-/-

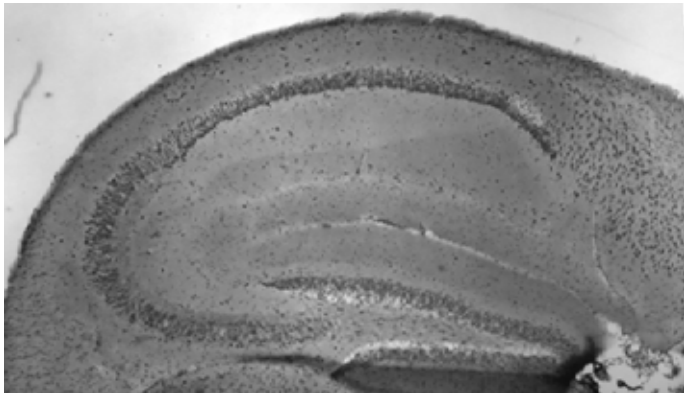

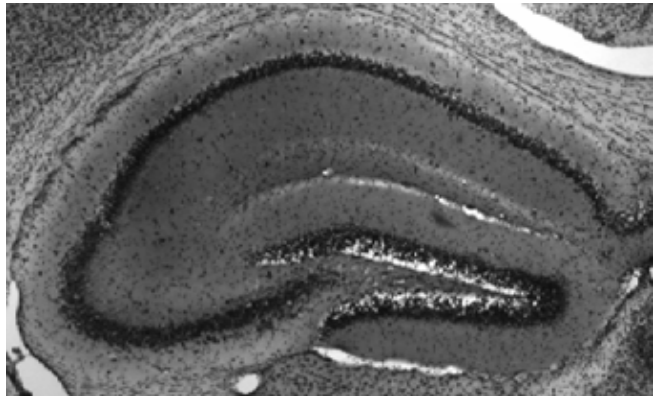

Figure 3

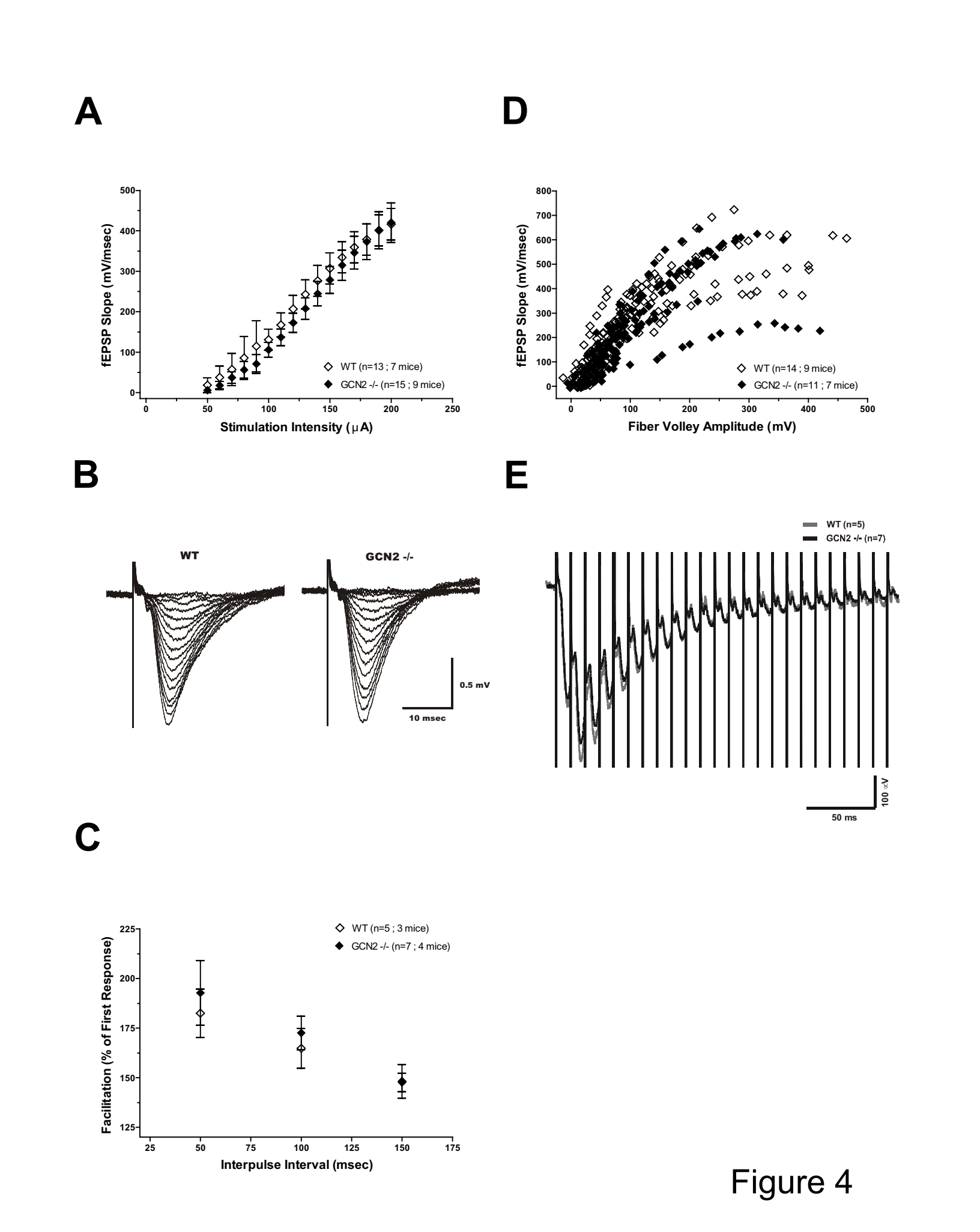
A
fEPSP Slope (mV/msec)
Stimulation Intensity (μA)
WT (n=13 ; 7 mice)
GCN2 -/- (n=15 ; 9 mice)
D
fEPSP Slope (mV/msec)
Fiber Volley Amplitude (mV)
WT (n=14 ; 9 mice)
GCN2 -/- (n=11 ; 7 mice)
B
WT
GCN2 -/-
0.5 mV
10 msec
E
WT (n=5)
GCN2 -/- (n=7)
100 μV
50 ms
C
Facilitation (% of First Response)
Interpulse Interval (msec)
WT (n=5 ; 3 mice)
GCN2 -/- (n=7 ; 4 mice)

Figure 4

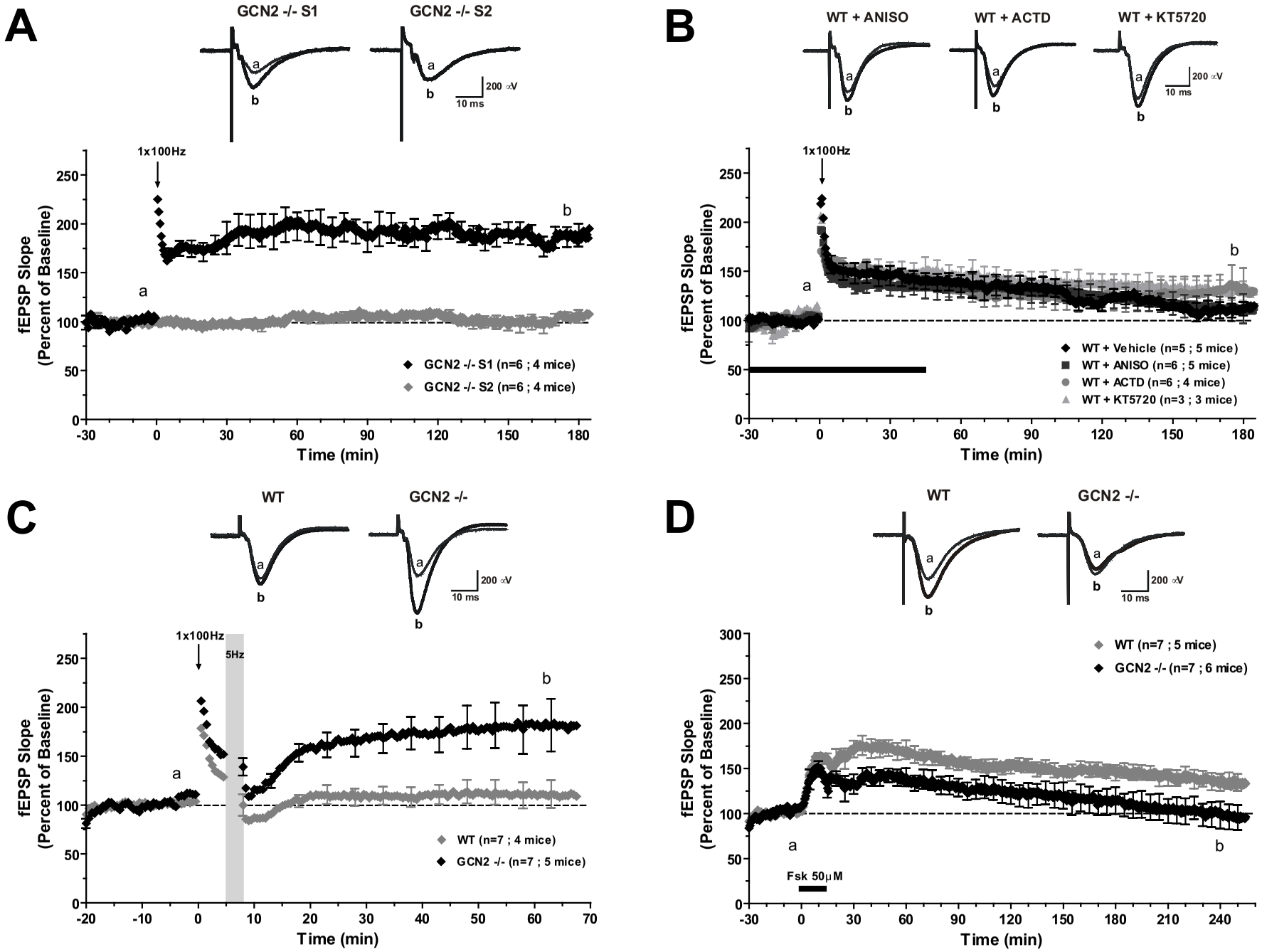
A
GCN2 -/- S1
GCN2 -/- S2
a
b
200 ∝V
10 ms
1x100Hz
fEPSP Slope
(Percent of Baseline)
Time (min)
GCN2 -/- S1 (n=6 ; 4 mice)
GCN2 -/- S2 (n=6 ; 4 mice)
B
WT + ANISO
WT + ACTD
WT + KT5720
WT + Vehicle (n=5 ; 5 mice)
WT + ANISO (n=6 ; 5 mice)
WT + ACTD (n=6 ; 4 mice)
WT + KT5720 (n=3 ; 3 mice)
C
WT
GCN2 -/-
5Hz
WT (n=7 ; 4 mice)
GCN2 -/- (n=7 ; 5 mice)
D
WT (n=7 ; 5 mice)
GCN2 -/- (n=7 ; 6 mice)
Fsk 50µM

Figure 5

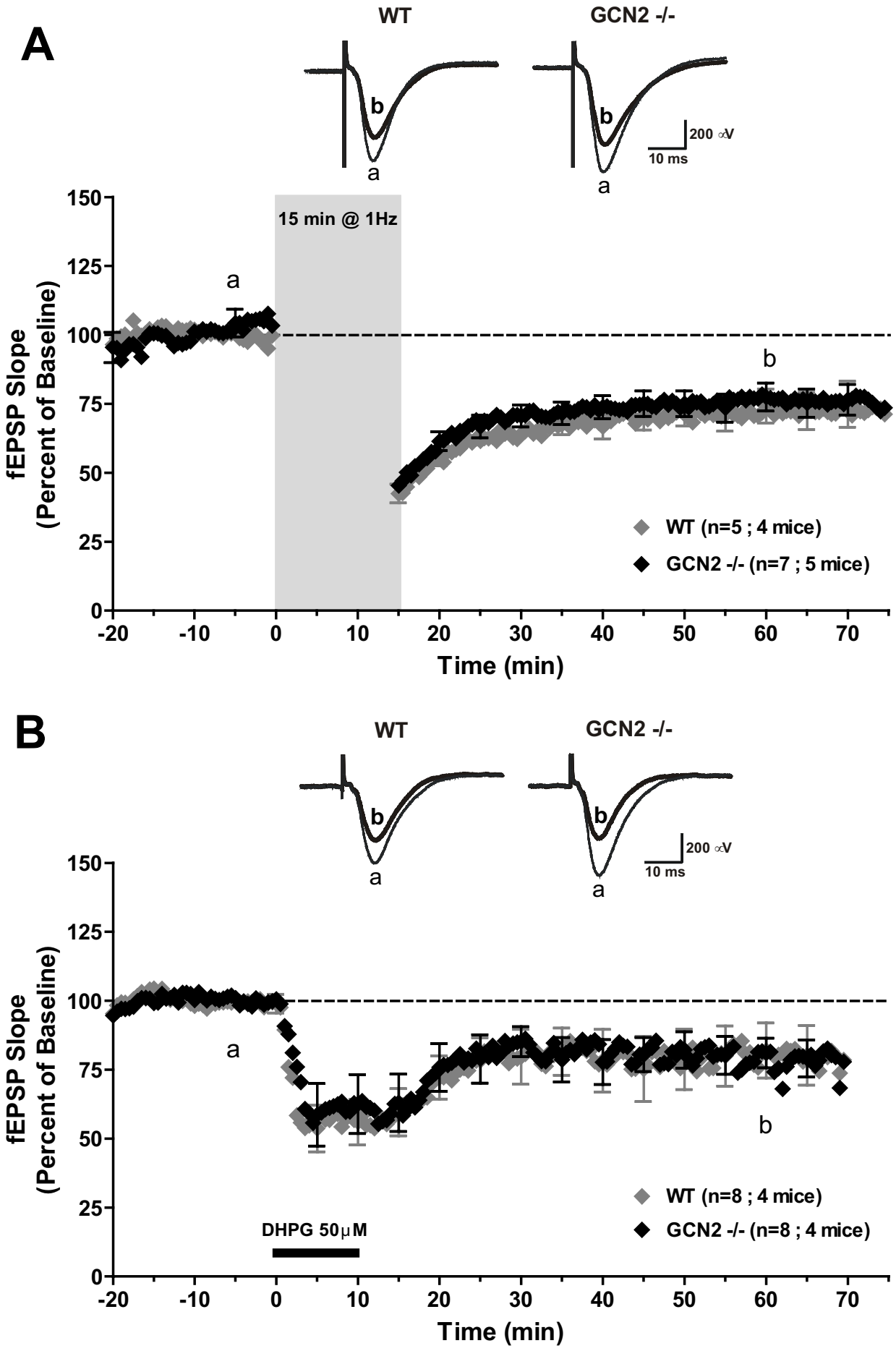
A
WT
GCN2 -/-
b
a
200 ∝V
10 ms
15 min @ 1Hz
fEPSP Slope
(Percent of Baseline)
Time (min)
WT (n=5 ; 4 mice)
GCN2 -/- (n=7 ; 5 mice)
B
WT
GCN2 -/-
DHPG 50µM
WT (n=8 ; 4 mice)
GCN2 -/- (n=8 ; 4 mice)

Figure 6

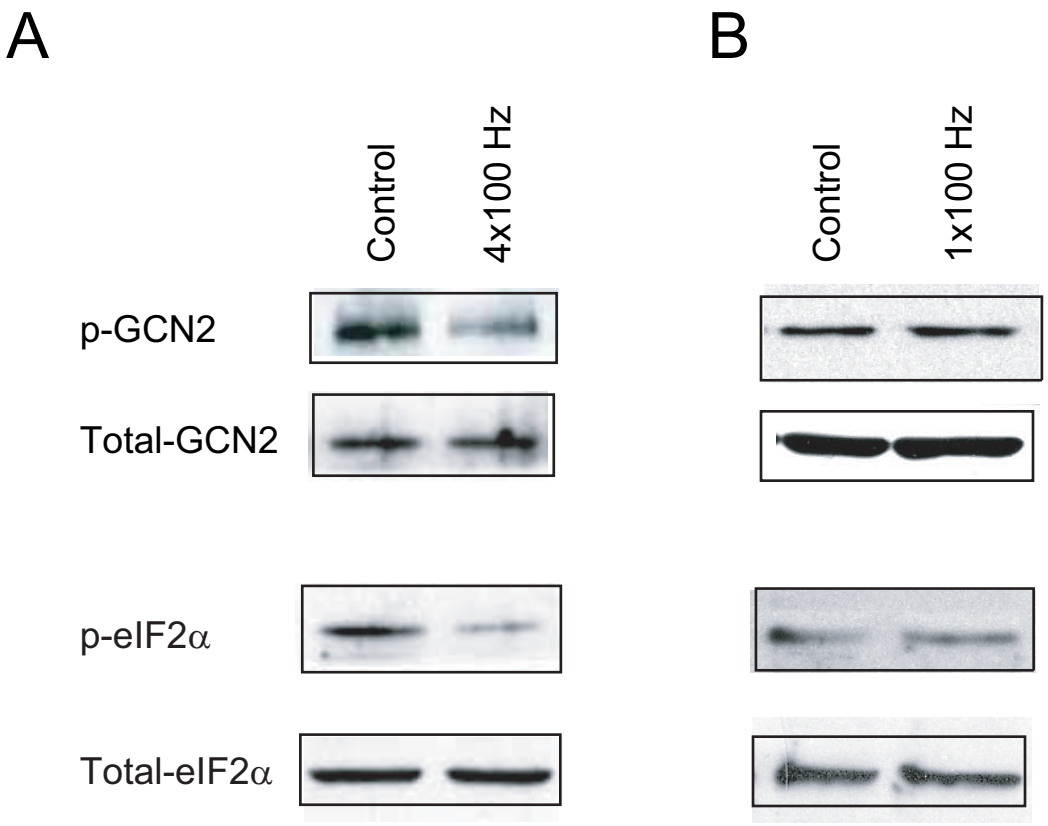
A
Control
4x100 Hz
p-GCN2
Total-GCN2
p-eIF2α
Total-eIF2α
B
Control
1x100 Hz

Figure 7